A consolidated method for predicting laminar boundary layers on rotating axi-symmetric bodies

Tobias Backer Dirks[1] and Chris Atkin[1]

[1]School of Mathematics, Computer Science & Engineering; City, University of London, 10 Northampton Square, London EC1V 0HB, UK

September 2018

Abstract

The boundary layer equations for axi-symmetric laminar flow are transformed in a manner which can be applied to rotating bodies in both still and axial flow. Terms pertaining specifically to quiescent or axial flow are clearly identified by the approach. The transformed equations are shown to deliver the same velocity profiles as a number of case-specific formulations presented in the literature, albeit with one or two exceptions, while being substantially simpler in formulation.

1 Introduction

Three dimensional boundary layers on rotating axi-symmetric bodies have long been the subject of much interest due to their similarity to the three dimensional boundary layers generated by flow over a swept wing. The seminal work of von Kármán (1921) looked at the boundary layer generated by a rotating disk in still air. His work was continued by Cochran (1934), who provided the first numerical results, and were later improved on by Benton (1966). A more general form of a rotating body of revolution was investigated by Schlichting (1953). In this he used a shape parameter K, analogous to the λ of the Pohlhausen method of boundary layer approximation, to try to generate solutions for a general axi-symmetric body. Schlichting's method is limited to cases with an imposed axial flow. Malik and Spall (1991) present the compressible boundary layer equations for an axi-symmetric body in an imposed axial flow making use of the Mangler-Levy-Lees transformation, in a similar fashion as in the present paper. However, their formulation is also limited to cases with an axial flow and rotation is not considered. Others have carried out analysis on well defined shapes using shape specific formulations of the governing equations. For example, Wu (1959) and Tien (1960) extended the case of a rotating disk to that of an axi-symmetric

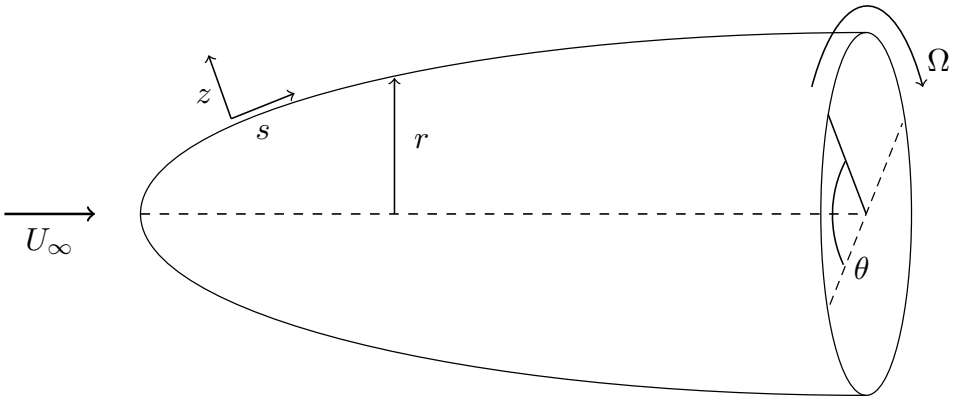

Figure 1: Sketch of the co-ordinate system for generalised body of revolution.

rotating cone in still air. The case of a rotating cone in an imposed axial flow was worked on by Koh and Price (1967), who made use of the similarity transforms of Mangler (1945). The boundary layer generated by a rotating sphere in still air was first investigated theoretically by Howarth (1951), and then Banks (1965) used a series solution method suggested by the former to generate boundary layer profiles. Following this, Manohar (1967) and Banks (1976) used more accurate finite difference techniques to resolve better the boundary layer of the rotating sphere. For the case of a rotating sphere in an imposed axial flow, El-Shaarawi et al. (1985) generated the first profiles based on the equations of Schlichting (1953).Finally, the work by Howarth (1951) on a rotating sphere in still air was extended by Fadnis (1954) to include prolate and oblate spheroids of different eccentricities using a series solution. Samad and Garrett (2010, 2014) then produced results from both series solution and finite difference techniques.

In more recent years interest has shifted towards the stability and transition of the boundary layers on rotating axi-symmetric bodies. The role of an absolute instability in the transitional boundary layer has been investigated for a rotating disk (Lingwood, 1995), a rotating cone in still air (Garrett, 2002; Garrett et al., 2009), a rotating cone in an axial flow (Garrett, 2002; Garrett and Peake, 2007; Garrett et al., 2010; Hussain, 2010), a rotating sphere in still air (Garrett, 2002; Garrett and Peake, 2002), a rotating sphere in an axial flow (Garrett, 2002; Garrett and Peake, 2004) and for prolate & oblate spheroids (Samad and Garrett, 2014). Accurate boundary layer profiles are a prerequisite for such stability analyses. Given the variety of manipulations to be found in the literature, the present work looks to formulate a consolidated set of transformations for the boundary layer equations on a general rotating body of revolution both in still air and in an axial flow, and to validate numerical solutions of these equations for a range of shapes and flow conditions.

2 Mathematical formulation

The governing equations (1a–c) were derived by Mangler (1945) for a rotationally symmetric flow past a body of revolution in a spherical co-ordinate system. u, v, w are velocity components in the directions of increasing s, θ and z as shown in figure 1.

$$\frac{\partial}{\partial s}(ru) + \frac{\partial}{\partial z}(rw) = 0, \tag{1a}$$

$$u\frac{\partial u}{\partial s} + w\frac{\partial u}{\partial z} - \frac{v^2}{r}\frac{\partial r}{\partial s} = u_e\frac{\partial u_e}{\partial s} + \nu\frac{\partial^2 u}{\partial z^2}, \tag{1b}$$

$$u\frac{\partial v}{\partial s} + w\frac{\partial v}{\partial z} + \frac{uv}{r}\frac{\partial r}{\partial s} = \nu\frac{\partial^2 v}{\partial z^2} \tag{1c}$$

In a fixed frame of reference these are subject to the boundary conditions

$$u = v - r\Omega = w = 0 \qquad \text{at} \quad z = 0 \tag{2a}$$

$$\begin{cases} u - u_e = v = 0, & u_\infty \neq 0 \\ u = v = 0, & u_\infty = 0 \end{cases} \qquad \text{as} \quad z \to \infty \tag{2b}$$

We define a two-component stream function

$$u = \frac{1}{r}\frac{\partial \psi}{\partial z}, \quad v = \frac{1}{r}\frac{\partial \phi}{\partial z}, \quad w = -\frac{1}{r}\frac{\partial \psi}{\partial s}, \tag{3a–c}$$

which satisfies the continuity equation (1a) and which allows a consistent treatment of the azimuthal velocity component v. We then define ψ and ϕ as functions of dimensionless stream functions f and g,

$$\psi = ru^* L_\xi f(\xi, \eta), \qquad \phi = r^2 \Omega L_\xi g(\xi, \eta), \tag{4a, b}$$

whereL_ξ is a viscous length scale and u^* is a switchable velocity scale of the form

$$u^* = \begin{cases} u_e, & u_\infty \neq 0 \\ r\Omega, & u_\infty = 0. \end{cases} \tag{5}$$

Using a variation of the Mangler-Levy-Lees transformation, a right-handed co-ordinate system is defined in which

$$\eta = \frac{z}{L_\xi}, \qquad L_\xi = \frac{\sqrt{2\xi}}{u^*}, \tag{6a, b}$$

$$\xi = \int \xi_s ds, \qquad \xi_s = \nu u^*., \tag{6c, d}$$

Substituting these transformations into equations (3a–c) yields

$$u = u^* f', \qquad v = r\Omega g', \tag{7a, b}$$

$$w = -\frac{u^*\nu}{\sqrt{2\xi}}\left[(\alpha+1)f - \eta(1-\gamma)f' + 2\xi\frac{\partial f}{\partial \xi}\right], \tag{7c}$$

where a prime denotes differentiation with respect to η. Inserting (7a–c) in to the governing equations (1a–c) ultimately yields

$$\begin{aligned} f''' \;+\; (\alpha+1)ff'' \;+\; \alpha\zeta g'^2 \;-\; \gamma f'^2 \;+\; \beta & \\ = \; 2\xi\left[\frac{\partial f'}{\partial \xi}f' \;-\; \frac{\partial f}{\partial \xi}f''\right], & \end{aligned} \tag{8a}$$

$$\begin{aligned} g''' \;+\; (\alpha+1)fg'' \;-\; 2\alpha f'g' & \\ = \; 2\xi\left[\frac{\partial g'}{\partial \xi}f' \;-\; \frac{\partial f}{\partial \xi}g''\right]. & \end{aligned} \tag{8b}$$

where the coefficients are

$$\alpha \;=\; \frac{2\xi}{r}\frac{\partial r}{\partial \xi}, \qquad \beta \;=\; \frac{2\xi u_e}{u^{*2}}\frac{\partial u_e}{\partial \xi}, \tag{9a, b}$$

$$\gamma \;=\; \frac{2\xi}{u^*}\frac{\partial u^*}{\partial \xi}, \qquad \zeta = \left(\frac{r\Omega}{u^*}\right)^2. \tag{9c, d}$$

The coefficient α relates to the shape of the body, β encompasses the streamwise slip velocity distribution ($\beta = 0$ in still air), while ζ is the square of the ratio of rotational velocity to streamwise velocity ($\zeta = 1$ in still air). Finally, γ is the term that allows us to switch the equations between their still and axial flow forms,

$$\gamma = \begin{cases} \beta, & u_\infty \neq 0 \\ \alpha, & u_\infty = 0. \end{cases} \tag{10}$$

Equations (8a,b) are subject to the following non-dimensional boundary conditions

$$f = f' = g = g' - 1 = 0 \qquad \text{at} \quad \eta = 0 \tag{11a}$$

$$\begin{cases} f' - 1 = g' = 0, & u_\infty \neq 0 \quad \text{as} \quad \eta \to \infty \\ f' = g' = 0, & u_\infty = 0 \end{cases} \tag{11b}$$

3 Solution and verification of the general equations

Equations (8a,b) can be reduced to a system of partially-coupled linear ordinary differential equations by employing a finite difference expression for the ξ-derivatives. This system is parabolic in character so that upwind differencing can be used, resulting in a system of local ordinary differential equations at any given ξ. In the present work, these are solved using a 4^{th} order compact-difference scheme on a stretched η mesh, with near-wall $\Delta\eta = 0.02$, a stretch factor of 1.1 and a total of 29 points for $0 < \eta < 6$. The coefficients defined by equations (9a,b) are obtained by numerical differentiation of the relevant geometry and the associated inviscid solution, here obtained using an axi-symmetric vortex sheet method (which is not described in this paper) except for self-similar cases.

In order to establish the validity of the proposed equations, results were compared with published velocity profiles for a variety of shapes and flow conditions.

3.1 Rotating disk in still air

The equations for the mean flow of a rotating disk in still air as derived by von Kármán (1921) are

$$f''' + 2ff'' + g'^2 - f'^2 = 0, \tag{12a}$$

$$g''' + 2fg'' - 2f'g' = 0, \tag{12b}$$

where in his formulation

$$u = r\Omega f'(\eta), \quad v = r\Omega g'(\eta), \tag{13a, b}$$

$$w = -2\sqrt{\nu\Omega} f(\eta), \quad \eta = z\sqrt{\frac{\Omega}{\nu}}. \tag{13c, d}$$

We have confirmed that equations (12a,b) can be obtained by manipulating equations (8a,b) by switching to the η defined in equation (13d) above and by substituting $s = r$ in equations (3c) and (6c). Comparison of the velocity profiles calculated by the present method with those generated by Benton (1966) using von Kármán's formulation, figure 2, also demonstrates that the present numerical scheme resolves the velocity profiles in the η direction with acceptable accuracy.

3.2 Rotating cone

3.2.1 Still air

The equations for the mean flow of a rotating cone of half-angle ψ in still air were derived by Wu (1959) and Tien (1960). Their formulation maintains the

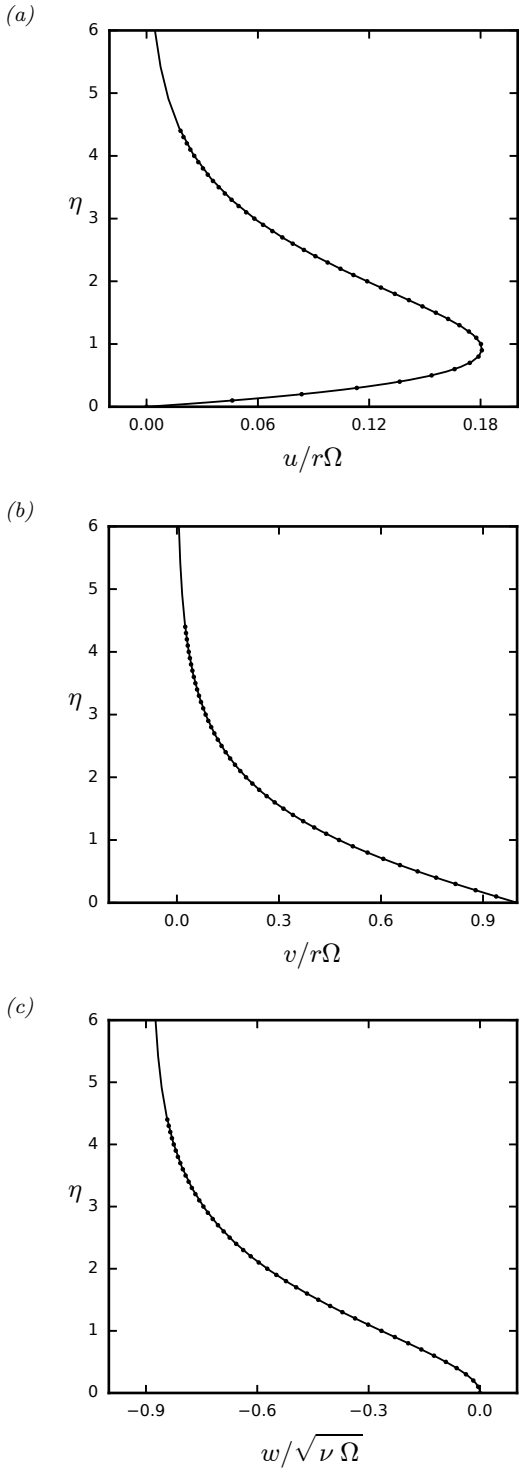

Figure 2: Comparison of the velocity profiles on a rotating disk, obtained using the present approach, with those reported by Benton (1966) ($\cdot$); η as defined in equation (13d).

same form of the boundary layer equations as for a rotating disk, while including the cone half-angle ψ within the wall-normal co-ordinate η. This is achieved in the present method through the inclusion of the local radius r in the velocity scale u^* which is present in our transformed wall-normal co-ordinate, equations (5) and (9a–d). Garrett (2002), in an effort to match more readily experimental Reynolds numbers, includes ψ direction in the boundary-layer equations (14a,b) rather than including it in the wall-normal co-ordinate, thereby maintaining the same η scaling and as in the case of the rotating disk, equation (13d),

$$f''' + \left(2ff'' + g'^2 - f'^2\right)\sin\psi = 0, \tag{14a}$$

$$g''' + (2fg'' - 2f'g')\sin\psi = 0, \tag{14b}$$

Other definitions are as in equations (13a,b) above, noting that the wall-normal velocity component for the cone is given by

$$w = -2\sin\psi\sqrt{\nu\Omega}f(\eta) \tag{15}$$

Equations (8a,b) can be manipulated as for the disk case, but using $r = s\ \sin\ \psi$ to obtain equations (14a,b). Comparison of the velocity profiles calculated by the present method with those generated by Garrett (2002) for the rotating cone in still air, figure 3, validates our more general formulation of the boundary layer equations.

3.2.2 Imposed axial flow

Koh and Price (1967) derived the mean flow equations for a rotating cone in an axial flow. In this case there exists no similarity transformation to reduce the mean flow equations from partial differential equations to a set of ordinary differential equations. Koh's approach assumes a power law for the boundary layer edge velocity, u_e, and incorporates this in the transformations, causing the boundary layer equations to take on a more complex form,

$$\begin{aligned} f''' + ff'' &+ \frac{2m}{m+3}(1-f'^2) \\ &+ \frac{2\xi}{m+3}\left[g'^2 + 2(1-m)\left(\frac{\partial f}{\partial \xi}f'' - \frac{\partial f'}{\partial \xi}f'\right)\right] = 0, \end{aligned} \tag{16a}$$

$$\begin{aligned} g''' + fg'' &- \frac{4}{m+3}f'g' \\ &+ \frac{4(1-m)\xi}{m+3}\left(\frac{\partial f}{\partial \xi}g'' - \frac{\partial g'}{\partial \xi}f'\right) = 0. \end{aligned} \tag{16b}$$

m depends only on the angle ψ. The non-dimensional velocity components are given by

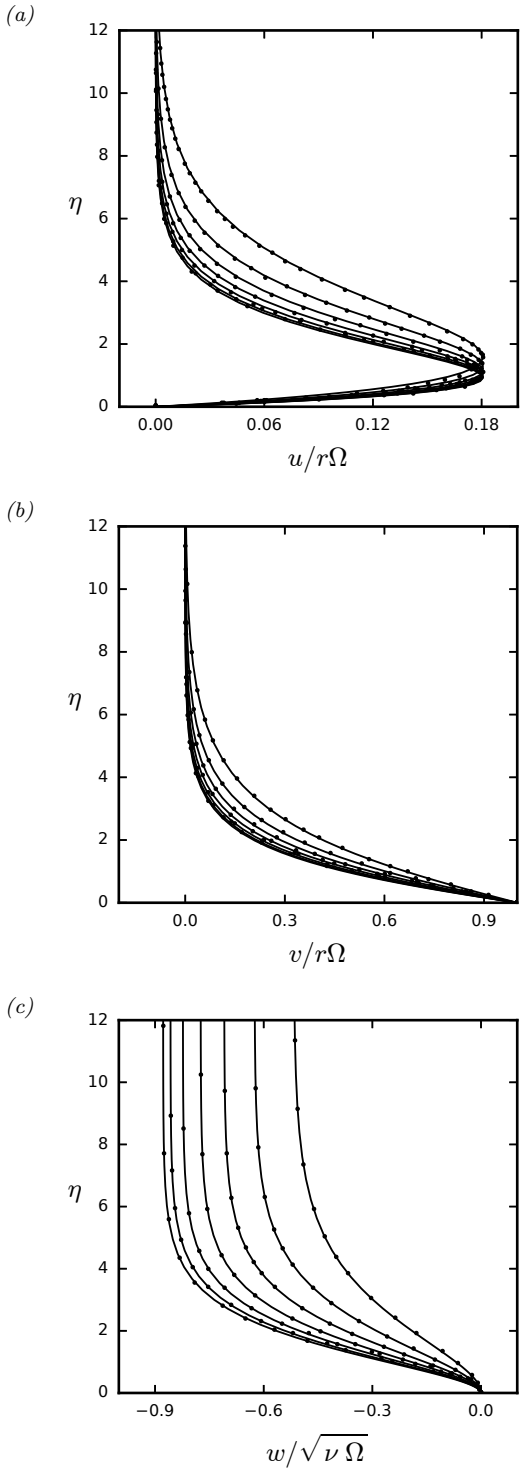

Figure 3: Comparison of the velocity profiles on a rotating cone (in still air) of half-angle $\psi = 20^\circ \rightarrow 80^\circ$ in 10° increments (right to left), obtained using the present approach, with those reported by Garrett (2002) ($\cdot$); η as defined in equation (13d).

$$u = \bar{u}_e f'(\xi,\eta), \qquad v = \omega \bar{x}^{1/3}\, g'(\xi,\eta), \tag{17a, b}$$

$$w = -\left(\frac{6}{m+3}\nu\bar{x}\bar{u}_e\right)^{1/2}\left[\left(\frac{1}{2\bar{x}}+\frac{1}{2\bar{u}_e}\right) f(\xi,\eta) + \frac{\partial\xi}{\partial\bar{x}}\frac{\partial f}{\partial\xi} + \frac{\partial\eta}{\partial\bar{x}} f'\right], \tag{17c}$$

where

$$\xi \;=\; \left(\frac{\bar{v}_w}{\bar{u}_e}\right)^2 = \left(\frac{\omega}{\bar{b}}\bar{x}^{(1-m)/3}\right)^2, \quad \eta \;=\; \bar{z}\left(\frac{m+3}{6}\frac{\bar{u}_e}{\nu\bar{x}}\right)^{1/2}, \tag{18a, b}$$

$$\omega \;=\; \Omega\left(3l^2 \sin\psi\right)^{1/3}. \tag{18c}$$

and where l is an arbitrary length scale, b is a flow constant and the transformed length scales and edge velocity are

$$\bar{x} \;=\; \frac{1}{l^2}\int_0^s r^2 ds, \qquad \bar{z} \;=\; \frac{r}{l}\, z, \qquad \bar{u}_e \;=\; b\bar{x}^{m/3}. \tag{19a–c}$$

Equations (8a,b) can be manipulated using $r = s\sin\psi$, defining the velocity scale $u^* = u_e = b\, s^m$ and adopting η as in equation (18b) to obtain equations (16a,b). Comparison of the profiles obtained from the present finite-difference method with those generated by Koh and Price (1967) for the rotating cone in an axial flow, figure 4, confirms that the velocity derivatives are correctly captured in our approach. Differences in v are attributed to a reduced resolution in the source image from which results were digitised. However the agreement with the velocity profiles published by Garrett et al. (2010), figure 5, is not good, particularly in the u-component near $\eta = 1$. The approach adopted by Garrett et al. (2010), an adaptation of the method of Koh and Price (1967), aimed to address limitations in the results presented in Garrett (2002), from which we also differ. A key point is the non-monotonic development of the u-velocity peak in the streamwise direction, highlighted by Hussain (2010, p28) but not present in our results, nor indeed in Garrett's analysis of the rotating sphere problem, Garrett (2002).

3.3 Rotating sphere

3.3.1 Still air

The equations for the boundary layer of a rotating sphere in still air, first investigated by Howarth (1951), are shown here as formulated by Manohar (1967),

$$f''' \;+\; \left(ff'' + g'^2\right)\cot\theta \;=\; \left[f'\frac{\partial f'}{\partial\theta} - f''\frac{\partial f}{\partial\theta}\right] \tag{20a}$$

$$g''' \;+\; \left(fg'' + f'g'\right)\cot\theta \;=\; \left[f'\frac{\partial g'}{\partial\theta} - g''\frac{\partial f}{\partial\theta}\right], \tag{20b}$$

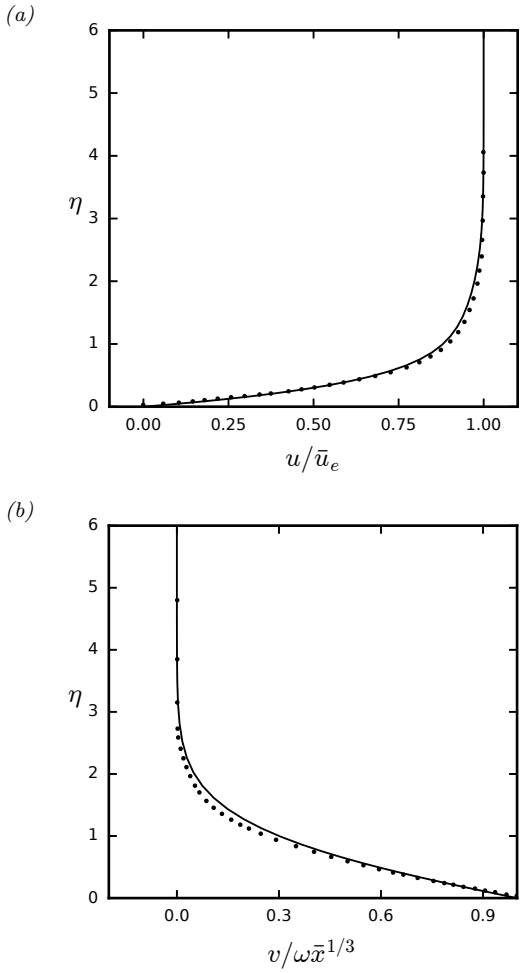

Figure 4: Comparison of the velocity profiles on a rotating cone (in an axial flow) of half-angle $\psi = 53.5^\circ$ and $\xi = 10$, obtained using the present approach, with those reported by Koh and Price (1967) ($\cdot$); η as defined in equation (18b).

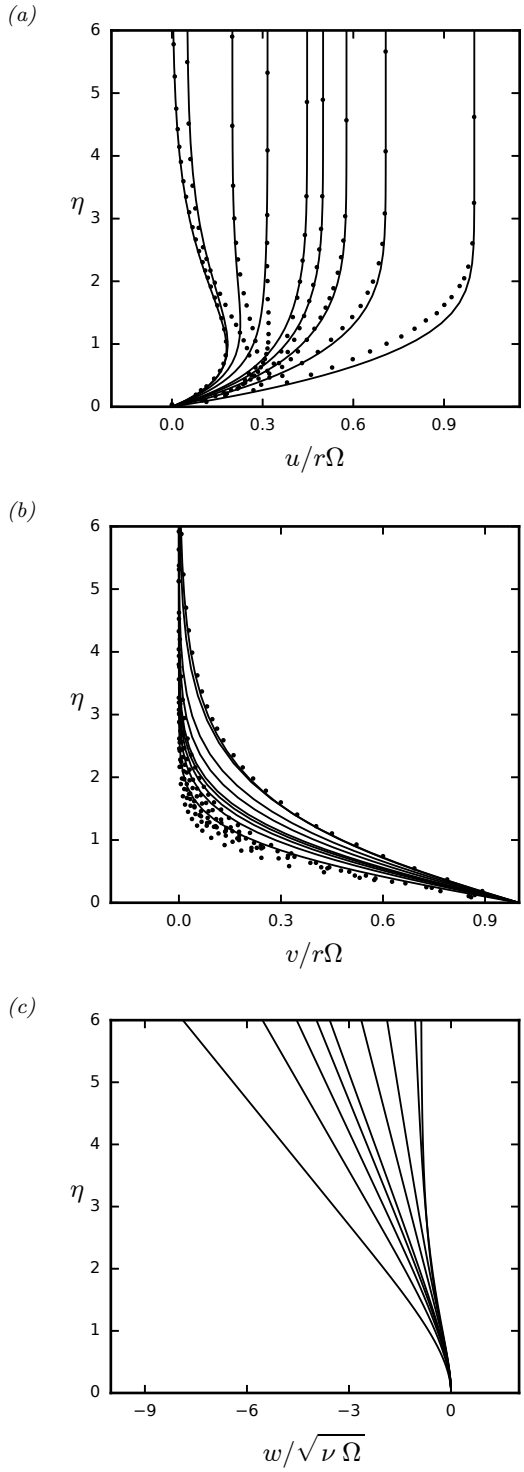

Figure 5: Comparison of the velocity profiles on a rotating cone (in an axial flow) of half-angle $\psi = 70^\circ$ and $\xi = 1, 1, 2, 3, 4, 5, 10, 25, 400$ and ∞ (right to left), obtained using the present approach, with those reported by Garrett et al. (2010) and Hussain (2010) ($\cdot$); η as defined in equation (13d).

where θ is the angle of latitude measured from the axis of rotation, the wall-normal co-ordinate η is as defined in equation (13d) and non-dimensional velocity components are given by

$$u = r_0 \Omega f'(\eta, \theta), \quad v = r_0 \Omega g'(\eta, \theta), \tag{21a, b}$$

$$w = -\sqrt{\nu \Omega} \left(\cot\theta f(\eta, \theta) + \frac{\partial f}{\partial \theta} \right). \tag{21c}$$

where r_0 is the radius of the sphere. Equations (20a,b) can be obtained from (8a,b) by using $r = r_0 \sin\theta$, $s = r\theta$ and adopting η as defined in equation (13d). Figure 6 presents a comparison of the velocity profiles computed using the present approach with those generated by Garrett (2002), Garrett and Peake (2002) and Segalini and Garrett (2017), who made use of the above formulation.

3.3.2 Imposed axial flow

The equations for the boundary layer of a rotating sphere in an axial flow were originally derived by El-Shaarawi et al. (1985) and are shown here as presented by Garrett (2002)

$$f''' + \left(ff'' + g'^2\right)\cot\theta + T_s^2 u_0 \frac{\partial u_0}{\partial \theta} = \left[f' \frac{\partial f'}{\partial \theta} - f'' \frac{\partial f}{\partial \theta} \right] \tag{22a}$$

$$g''' + \left(fg'' + f'g'\right)\cot\theta = \left[f' \frac{\partial g'}{\partial \theta} - g'' \frac{\partial f}{\partial \theta} \right] \tag{22b}$$

where θ is the angle of latitude measured from the axis of rotation, T_s is the ratio of free-stream axial flow velocity to rotational velocity, $T_s = u_\infty / r_0 \Omega$, and u_0 is a non-dimensionalised slip velocity, $u_0 = u_e / u_\infty$. The wall-normal co-ordinate η and stream function definitions maintain the same scaling as in the case of the rotating sphere in still air, equations (21a–c) and (13d). The transformation of equations (8a,b) to equations (22a,b) follows a similar approach to that described in section 3.3.1. The comparison of the results from present method with those generated by Garrett (2002) in figure 7, for $\theta = 10^\circ$ and figure 8, for $\theta = 70^\circ$ are again very good.

3.4 Rotating prolate spheroid in still air

The equations for the boundary layer of a rotating prolate spheroid in still air, first investigated by Fadnis (1954), are shown here as formulated by Samad and Garrett (2010),

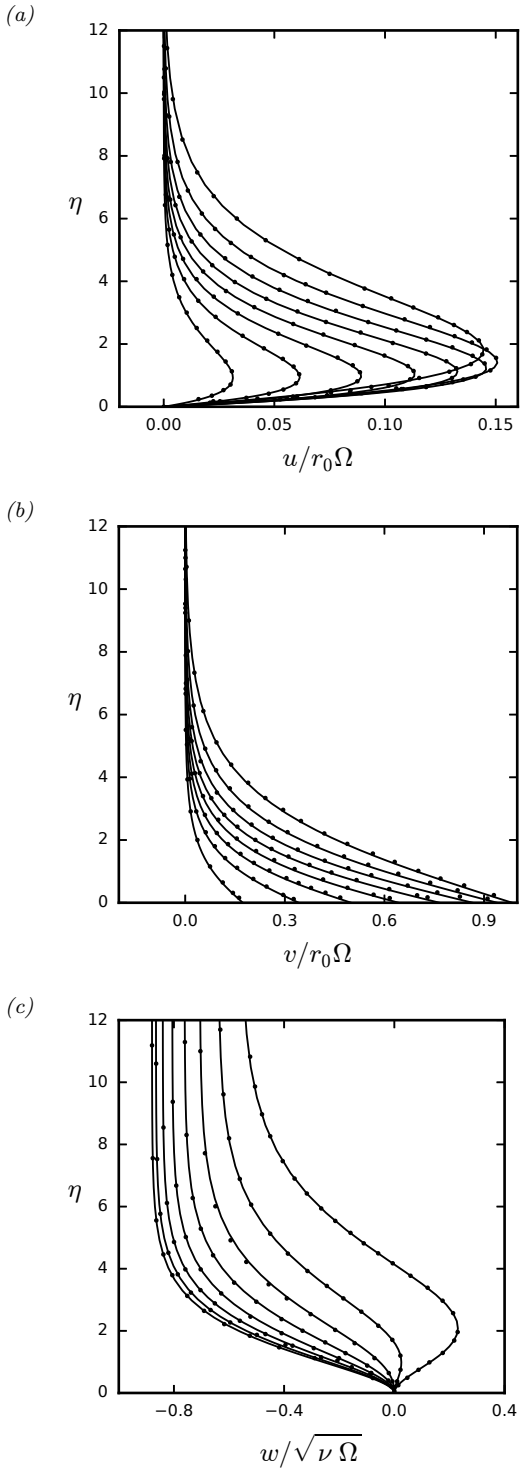

Figure 6: Comparison of the velocity profiles on a rotating sphere (in still air) at $\theta = 10^\circ \rightarrow 80^\circ$ in 10° increments (left to right), obtained using the present approach, with those reported by Garrett (2002), Garrett and Peake (2002) and Segalini and Garrett (2017) $(\cdot)$; η as defined in equation (13d).

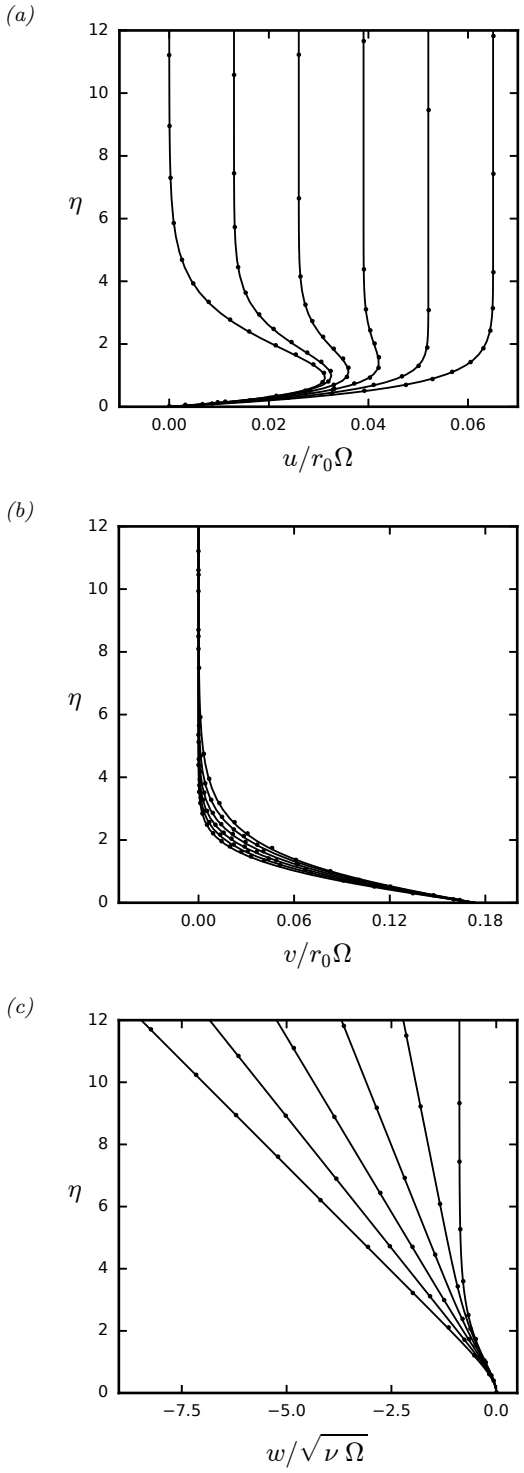

Figure 7: Comparison of the velocity profiles on a rotating sphere (in an axial flow) at $\theta = 10^\circ$ and $T_s = 0, 0.05, 0.1, 0.15, 0.2$ and 0.25 (left to right), obtained using the present approach, with those reported by Garrett (2002) ($\cdot$); η as defined in equation (13d).

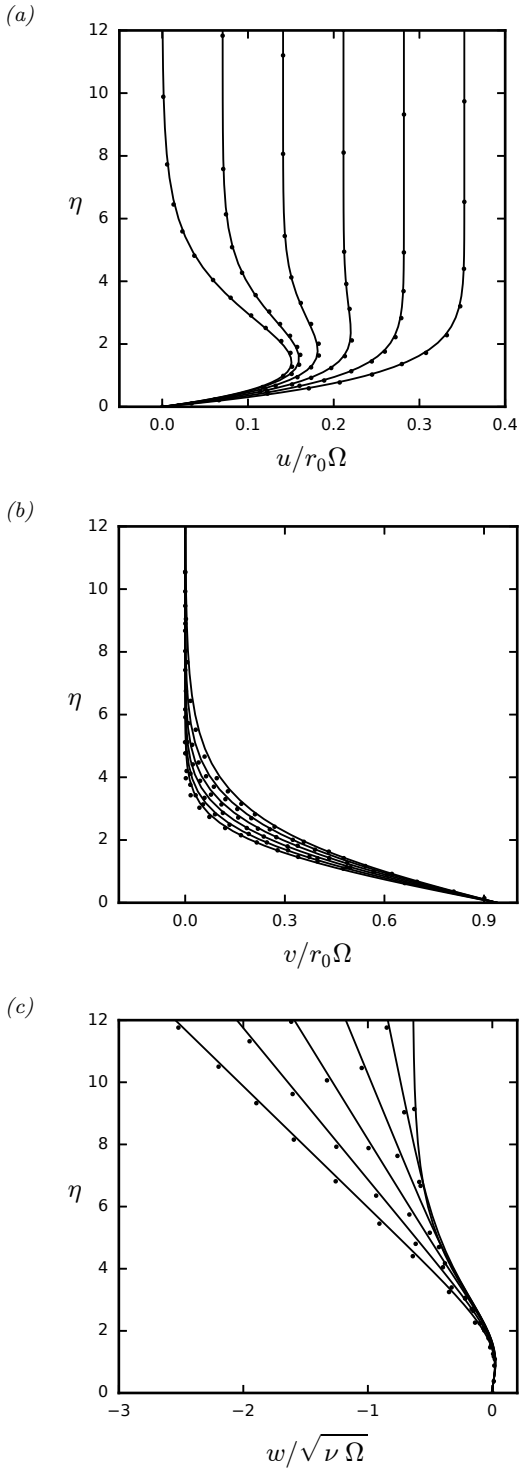

Figure 8: Comparison of the velocity profiles on a rotating sphere (in an axial flow) at $\theta = 70^\circ$ and $T_s = 0, 0.05, 0.1, 0.15, 0.2$ and 0.25 (left to right), obtained using the present approach, with those reported by Garrett (2002) ($\cdot$); η as defined in equation (13d).

$$f'''\sqrt{\frac{1-e^2}{1-e^2\cos^2\theta}} \;+\; g'^2\cot\theta \\ +\;\left(\frac{e^2\cos\theta\sin\theta}{1-e^2\cos^2\theta}+\cot\theta\right)ff'' \;=\; \left[f'\frac{\partial f'}{\partial\theta} \;-\; f''\frac{\partial f}{\partial\theta}\right] \tag{23a}$$

$$g'''\sqrt{\frac{1-e^2}{1-e^2\cos^2\theta}} \;-\; f'g'\cot\theta \\ +\;\left(\frac{e^2\cos\theta\sin\theta}{1-e^2\cos^2\theta}+\cot\theta\right)fg'' \;=\; \left[f'\frac{\partial g'}{\partial\theta} \;-\; g''\frac{\partial f}{\partial\theta}\right] \tag{23b}$$

where θ is the angle of latitude measured from the axis of rotation in an elliptical co-ordinate system and e is the eccentricity of the ellipsoid. The wall-normal co-ordinate is defined as $\eta = (\Omega^*/\nu^*)^{1/2}(\eta^* - \eta_0^*)$, where * denotes dimensional quantities in his formulation and η^* and η_0^* are the total wall-normal distance from the axis of revolution and wall-normal distance from the axis of revolution to the surface of the spheroid, respectively. This should be analogous to η as defined in equation (13d). The non-dimensional velocity components u, v are defined as for the sphere in equation (21a,b) but w is given by

$$w = -\sqrt{\nu\Omega}\left[\left(\frac{e^2\cos\theta\sin\theta}{1-e^2\cos^2\theta}+\cot\theta\right)f(\eta,\theta)+\frac{\partial f}{\partial\theta}\right] \tag{24}$$

where here for a prolate spheroid r_0 is the maximum radial thickness, the length of the semi-minor axis. Due to the complex relation between r and s for a spheroid we have not verified that equations (8a,b) can be transformed to (23a,b). Nevertheless, velocity profiles calculated by the present method compare well with those generated by Samad and Garrett (2010) in figure 9 for $e = 0.3$; however, for the higher eccentricity case of $e = 0.7$, figure 10, the agreement, while good initially, is poor at increased latitude θ. The discrepancy appears to be connected with the different mapping of the η co-ordinates used by Samad and Garrett (2010, 2014) and in the present work, as the magnitudes of the peak velocities agree closely. There is some ambiguity in the definition of η_0^* between Samad and Garrett (2010) and Samad and Garrett (2014) which may explain the discrepancies at higher θ for large eccentricities. In former η_0^* is defined as the wall-normal distance to the surface from the axis of revolution while in the latter it is defined as the length of the semi-major axis. From this it would follow that differences would be greatest at higher eccentricities and latitudes. Unfortunately we were still unable to obtain a better match under these assumptions.

4 Conclusions

A generalised formulation of the boundary layer equations for an arbitrary rotating body of revolution has been presented. The use of a switchable velocity scale u^*, as well as the local radius r, within the transformations enables any

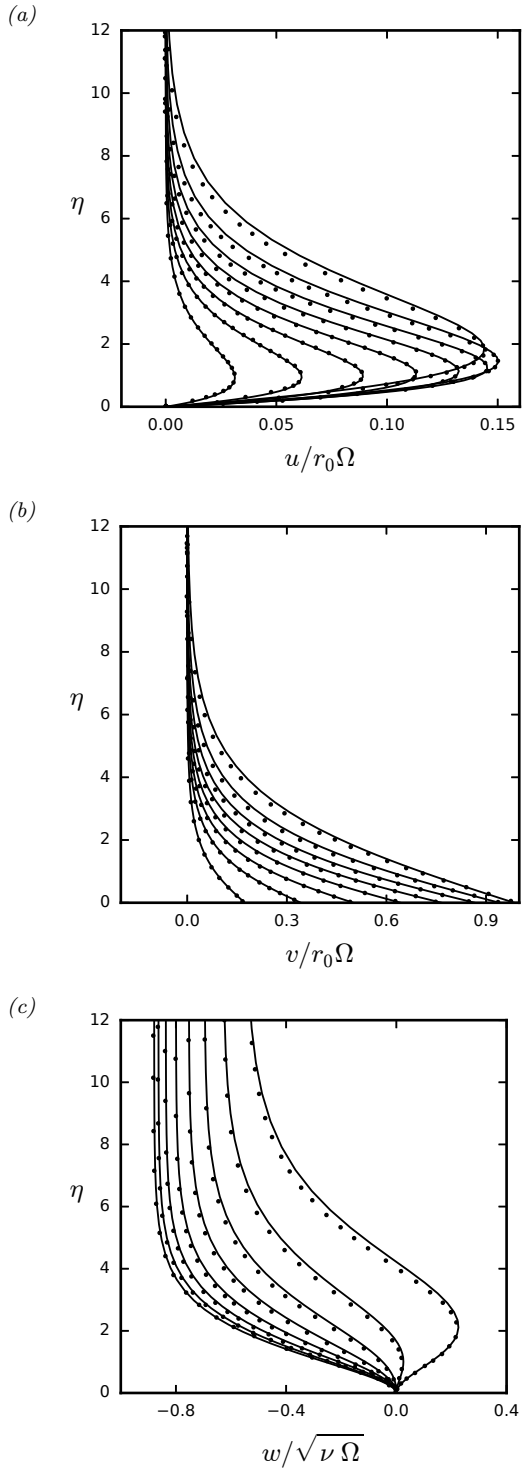

Figure 9: Comparison of the velocity profiles on a rotating prolate spheroid (in still air) with eccentricity 0.3 at $\theta = 10° \rightarrow 80°$ in 10° increments (left to right), obtained using the present approach, with those reported by Samad and Garrett (2010) ($\cdot$); η as defined in equation (13d).

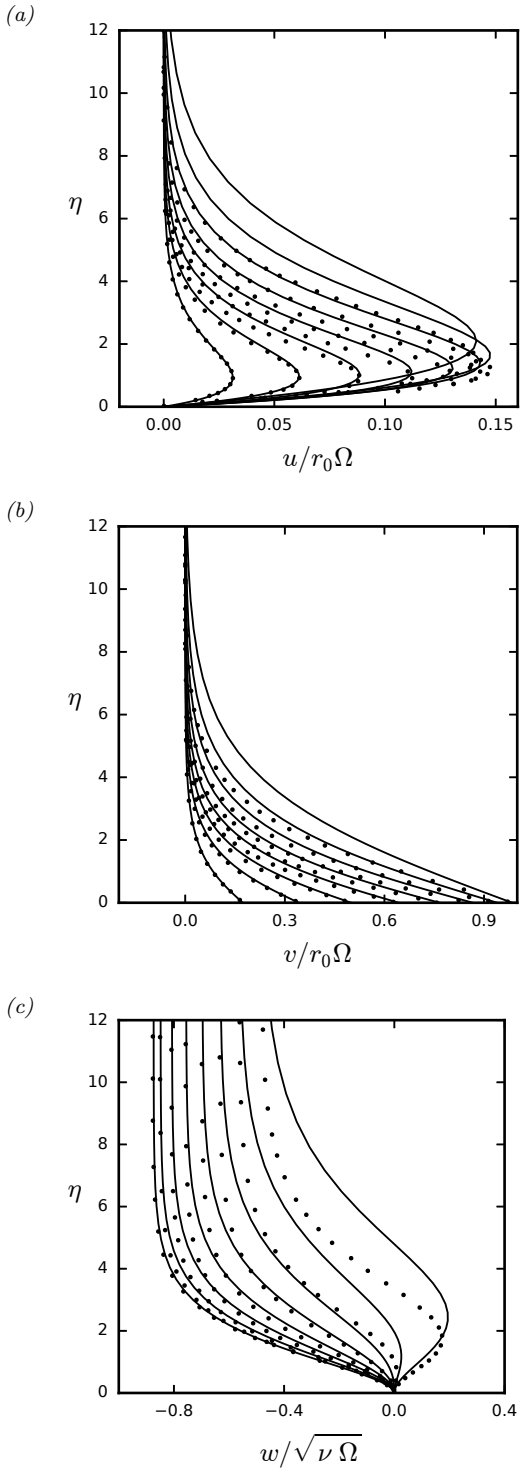

Figure 10: Comparison of the velocity profiles on a rotating prolate spheroid (in still air) with eccentricity 0.7 at $\theta = 10^\circ \rightarrow 80^\circ$ in 10° increments (left to right), obtained using the present approach, with those reported by Samad and Garrett (2010) ($\cdot$); η as defined in equation (13d).

rotating axi-symmetric body to be analysed, both with and without an axial flow. Comparisons with other published shape-specific formulations appear to confirm the validity of both the mathematical formulation and the numerical scheme employed, but there are some isolated discrepancies which remain to be resolved.

Acknowledgements

The authors would like to acknowledge the support of Airbus Group Innovations under agreement number AGI-102607.

References

T. von Kármán, Über laminare und turbulente reibung, ZAMM-Zeitschrift für Angewandte Mathematik und Mechanik 1 (1921) 233–252.

W. G. Cochran, The flow due to a rotating disc, in: Mathematical Proceedings of the Cambridge Philosophical Society, volume 30-3, Cambridge Univ Press, 1934, pp. 365–375.

E. R. Benton, On the flow due to a rotating disk, Journal of Fluid Mechanics 24 (1966) 781–800.

H. Schlichting, Die laminare strömung um einen axial angeströmten rotierenden drehkörper, Archive of Applied Mechanics 21 (1953) 227–244.

M. R. Malik, R. E. Spall, On the stability of compressible flow past axisymmetric bodies, Journal of fluid mechanics 228 (1991) 443–463.

C. S. Wu, The three dimensional incompressible laminar boundary layer on a spinning cone, Applied Scientific Research, Section A 8 (1959) 140–146.

C. L. Tien, Heat transfer by laminar flow from a rotating cone, Journal of Heat Transfer 82 (1960) 252–253.

J. C. Y. Koh, J. F. Price, Non-similar boundary layer heat transfer of a rotating cone in a forced flow., Journal of Heat Transfer 89 (1967) 139–145.

W. Mangler, Grenzschichten an Rotationskörpern bei symmetrischer Anblasung, number 45 in Bericht / A 17: Bericht, Göttingen Aerodynamische Versuchsanstalt, 1945. URL: `http://books.google.co.uk/books?id=QsCjtgAACAAJ`.

L. Howarth, Cxxix. note on the boundary layer on a rotating sphere, London, Edinburgh, and Dublin Philosophical Magazine and Journal of Science 42 (1951) 1308–1315.

W. H. H. Banks, The boundary layer on a rotating sphere, The Quarterly Journal of Mechanics and Applied Mathematics 18 (1965) 443–454.

R. Manohar, The boundary layer on a rotating sphere, Zeitschrift für Angewandte Mathematik und Physik (ZAMP) 18 (1967) 320–330.

W. H. H. Banks, The laminar boundary layer on a rotating sphere, Acta Mechanica 24 (1976) 273–287.

M. A. I. El-Shaarawi, M. F. El-Refaie, S. A. El-Bedeawi, Numerical solution of laminar boundary layer flow about a rotating sphere in an axial stream, Journal of Fluids Engineering 107 (1985) 97.

B. S. Fadnis, Boundary layer on rotating spheroids, Zeitschrift für Angewandte Mathematik und Physik (ZAMP) 5 (1954) 156–163.

A. Samad, S. J. Garrett, On the laminar boundary-layer flow over rotating spheroids, International Journal of Engineering Science 48 (2010) 2015–2027.

A. Samad, S. J. Garrett, On the stability of boundary-layer flows over rotating spheroids, International Journal of Engineering Science 82 (2014) 28–45.

R. J. Lingwood, Absolute instability of the boundary layer on a rotating disk, Journal of Fluid Mechanics 299 (1995) 17–33.

S. J. Garrett, The stability and transition of the boundary layer on rotating bodies, Ph.D. thesis, University of Cambridge, 2002.

S. J. Garrett, Z. Hussain, S. O. Stephen, The cross-flow instability of the boundary layer on a rotating cone, Journal of Fluid Mechanics 622 (2009) 209–232.

S. J. Garrett, N. Peake, The absolute instability of the boundary layer on a rotating cone, European Journal of Mechanics-B/Fluids 26 (2007) 344–353.

S. J. Garrett, Z. Hussain, S. O. Stephen, Boundary-layer transition on broad cones rotating in an imposed axial flow, AIAA Journal 48 (2010) 1184–1194.

Z. Hussain, Stability and transition of three-dimensional rotating boundary layers, Ph.D. thesis, University of Birmingham, 2010.

S. J. Garrett, N. Peake, The stability and transition of the boundary layer on a rotating sphere, Journal of Fluid Mechanics 456 (2002) 199–218.

S. J. Garrett, N. Peake, The stability of the boundary layer on a sphere rotating in a uniform axial flow, European Journal of Mechanics-B/Fluids 23 (2004) 241–253.

A. Segalini, S. J. Garrett, On the non-parallel instability of the rotating-sphere boundary layer, Journal of Fluid Mechanics 818 (2017) 288–318.